Initiation of Electro-Oxidation of CO on Pt Based Electrodes at Full Coverage Conditions Simulated by Ab Initio Electronic Structure Calculations

Barry D. Dunietz,*,†,‡ Nenad M. Markovic,‡ Phil N. Ross,‡ and Martin Head-Gordon†,‡

Department of Chemistry, University of California at Berkeley, Chemical Sciences Division, Lawrence Berkeley National Laboratory, Berkeley, California 94720

Received: December 20, 2003; In Final Form: March 25, 2004

CO electrooxidation on Pt-based electrodes is simulated by density functional calculations on cluster models. Recently, simple cluster models were used to identify a crucial intermediate species for the reaction. In this work, we address the problem of the initiation of the CO electrooxidation process by employing extended models. These extended models are aimed at representing the surface at full coverage, which is believed to be the condition of the physical system at reaction initiation. According to the models employed in this study, it is concluded that for the reaction to begin at reasonable strength of the potential bias a vacancy has to occur at a site adjacent to an adsorbed CO. Such vacancies can be produced either by the presence of surface defects or due to dynamical desorption of CO.

Introduction

The electrooxidation of CO on Pt based electrodes has been the focus of extensive experimental and computational research. Based on the available data, CO electrooxidation is believed to follow a Langmuir−Hinshelwood mechanism. Accordingly, an oxygen containing species formed on the electrode surface reacts with adsorbed CO to form CO_2.[1−3] A schematic description of this mechanism is provided by

$$CO_{ads} + OH_{ads} \rightarrow CO_2 + H^+(\text{solution}) + e^- \qquad (1)$$

However, a full understanding of the reaction mechanism is still lacking.

Previous theoretical studies of the reaction were mainly based on kinetic Ising models and dynamic Monte Carlo simulations.[4,5] These studies have provided a parametrized coarsed grained description of the system and insight into the kinetics of the reaction such as the formation of CO islands was obtained. Previous ab initio studies employing gas-phase quantum chemistry (QC) methodology added important energetic and structural understanding of CO adsorption at the atomic level.[6−8] However, these calculations do not attempt to investigate the mechanism of CO electrooxidation. Thus, the microscopical details of the reaction have remained elusive, until recently.

QC methodology has been useful in providing possible insight on the reaction mechanism. Recently, Anderson and Neshev have suggested the role of an intermediate complex in the reaction mechanism.[9] Their DFT study has reconfirmed their earlier findings based on semiempirical methodology.[3] However, the models used in these studies are too limited to describe reasonably the surface chemistry. For example, full geometry optimizations could not be included with these early models. Full geometry optimizations, however, are required to add validity to the predictions obtained by the calculations. Very recently, by means of ab initio QC calculations employing geometry optimizations, progress in that regard has been accomplished.[10]

In that recent study,[10] a simple cluster model with the minimal features needed for a faithful representation of the surface chemistry in the electro-chemical environment was formulated. The results obtained by this model validated the important role of an intermediate formed in the CO electrooxidation process. The success of the simple model to describe the reaction is encouraging. In this study, we further extend the models used in that calculation in order to address (and represent) more physically the actual chemical environment. The question of how electrooxidation begins on the surface, where a full layer of adsorbed CO is present, is considered.

Models and Methods

Within the chosen cluster models, we performed first principles density functional calculations. Full geometry optimizations of the adsorbed species allow us to find stable surface structures without any further approximations. We have employed the widely used B3LYP exchange-correlation functional[16,17] along with the Pople 6-31G basis set extended with the LANL2DZ[18] effective core potential (ECP) and double valence zeta basis for the Pt atoms. All calculations were performed using the Q-Chem suite of quantum chemistry programs[19] with an overall zero charge and singlet spin coupling. The predominant relativistic effects, which arise due to the large Pt atoms, are related to the core electrons. These core-size effects are treated through the use of ECPs within the basis set. Other smaller relativistic effects are neglected.

Basic Model. In our previous study concerning CO electrooxidation, we have employed a cluster model of the electrode−electrolyte system to obtain insight into the reaction mechanism.[10] A simplified model that contained just the minimal features necessary to describe electrooxidation was defined. Since the current study directly extends that model, we first briefly describe it.

In the basic model, the surface is represented by a cluster of a total of ten Pt atoms. Two center atoms are used to represent

* To whom correspondence should be addressed.
† University of California at Berkeley.
‡ Lawrence Berkeley National Laboratory.

10.1021/jp037951u CCC: $27.50
Published on Web 06/18/2004

a pair of adjacent atop sites. The remaining eight Pt atoms are the next neighbors of these atoms on the outmost surface layer. The two center atoms were used to represent sites adsorbed with the interacting species, CO and OH. It was established that this cluster is the minimal sized cluster required to obtain qualitative description of the adsorbed surface.[10] Smaller clusters upon geometry optimization have produced unphysical features and thus were found not to reperesent qualitatively well the surface. The 10 atom model, on the other hand, which was used to identify the intermediate, was also the first allowing full geometry optimizations of the adsorbate atoms on the constrained surface.

The adsorbed CO and OH and a water molecule representing the solution were allowed to relax in geometry optimizations. In addition, the influence of an applied field, simulating the functionality of the electrode potential, on the optimized geometry was monitored.[11−13] Within the model used, a positive field applied to the surface corresponds to charging the metal atoms negatively and charging the COOH complex positively. This also corresponds to applying a positive electrode potential in an experiment.

It was found that placing CO and OH on adjacent atop sites favors the formation of adsorbed COOH. The COOH was then considered as an intermediate species in the CO electrooxidation process. Transient optimized structures of the solvated adsorbed COOH under the influence of potential bias have been collected. These structures have demonstrated that beyond a threshold bias field CO oxidation from the intermediate COOH species occurs. Specifically, the proton is transferred from the adsorbed COOH species to a water molecule, leaving behind CO_2 on the surface. This clearly demonstrated the occurrence of CO electrooxidation. In addition, estimates for the reaction barrier were obtained where the barrier is shown to vanish above a certain bias potential.

Although the results obtained are highly suggestive, it is important to stress that the initial geometry used for starting the geometry optimizations is already very favorable to allow oxidation to occur. This is not necessarily the situation in the actual system. It is interesting to investigate the initiation of the reaction when full coverage of CO is assumed and the adsorbed oxygen containing species next to CO is yet to be produced. In the next section, we describe models aimed at describing such actual physical conditions. Following that, we present the results and draw our conclusions on how the reaction can start when a full layer of CO is present.

Extended Models. Careful examination of recent experimental observations suggest that the reactivity of the adsorbed CO layer in the oxidation process stems from the CO species adsorbed on atop sites.[14,15] Hence, our models concentrate on describing the reactivity of these sites. Our previous model has been concentrated on the reactivity of two adjacent atop sites. In this study, we extend the previous model to better represent the actual environment without modifying the reactive core of the model.

In the extended model, we include additional CO adsorbates to simulate the full coverage of the surface. We approximate the influence of the neighboring adsorbed CO species at full coverage conditions by constraining these additional CO adsorbates to the adjacent atop sites. Thus, the rigid piece of the model now includes in addition to the ten Pt surface atoms eight CO molecules adsorbed on the cluster edge Pt atoms surrounding the two center atop sites.

In addition, the oxygen containing species is not readily provided as in the previous study in the form of OH adsorbed on a neighbor site. Instead, additional water molecules are included in the model. These water molecules are allowed to interact with the adsorbed CO species and the surface under the influence of the field. We have calculated the potential energy surface (PES) under the influence of applied electric potential with increments of 0.13 V/Å fields (we have stepped the applied fields in 0.0025 a.u increments which translates to about 0.13 V/Å).

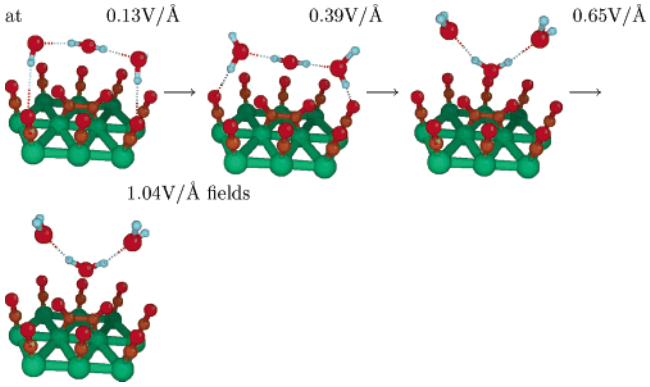

Figure 1. Extended models for full coverage with no empty site conditions. A slow approach to the adsorbed CO by water molecules is initially demonstrated. However, at above a certain potential, the three water molecules are repelled as a cluster away from the surface. This demonstrates the unfavorable conditions for the reaction to occur. In all figures, Pt atoms are represented with green circles, carbons with orange color, oxygens are colored red, and the hydrogens appear as light blue circles.

In our models, the origin of the oxygen needed for oxidation is assumed to be a water molecule. Thus, we include three explicit water molecules in the model. One molecule will supply the oxygen oxidizing CO, whereas the role of the two other molecules is to allow transfer of the hydrogens from the adsorbed species to the "bulk" of the solution. CO_2 is formed as the result of the oxidation process. These three water molecules address the minimum requirement for simulating the oxidation of the water molecules which possibly precedes its reaction with adsorbed CO a described above.

To assess how the reaction actually begins on the fully covered surface, several variants of the model have been tested. Different PESs with respect to the electric potential bias have been calculated in order to elucidate the conditions under which the reaction can start. Two possibilities have been considered. In the first scheme, water attacks directly the adsorbed CO under the influence of the potential bias. In the other scheme, it is assumed that water needs to first get adsorbed on the surface and only then can react with an adjacent adsorbed CO. This scheme assumes that a vacancy can be made available next to an adsorbed site even at full coverage. In reality, such vacancies can appear, either due to the dynamics of the system, where CO is constantly adsorbing and desorbing, or simply in a form of a surface defect. The importance of surface defects has been experimentally demonstrated by Lebedeva et al., where the electrooxidation reaction constant was shown to vanish at the limit of a perfect 111 crystal.[20] Computational modeling by studying the macroscopical features of the systems has also hinted to the role of vacancies or defects in the reaction mechaism.[4,5]

Results and Discussion

First we will consider the possibility of the reaction occurring when there is no vacancy available next to the reacting adsorbed CO molecule. Figure 1 shows the coordination of the attacking

TABLE 1: Charges of the Relaxed Atoms at Two Different Structures at 1.04 V/Å under Full Coverage Scenario[a]

atom	initial guess structure		relaxed structure	
energy (a.u.)	−2553.7359		−2553.7691	
Pt	−0.43		−0.40	
Pt	−0.42		−0.40	
C	0.17	−0.05	0.16	−0.09
O	−0.22		−0.25	
O	−0.66	0.22	−0.56	0.38
H	0.45		0.45	
H	0.45		0.47	
O	−0.72	0.17	−0.68	0.25
H	0.44		0.45	
H	0.45		0.47	
O	−0.74	0.14	−0.70	0.22
H	0.44		0.47	
H	0.44		0.45	
C	0.17	−0.05	0.17	−0.08
O	−0.22		−0.25	

[a] The first structure is the optimized structure at 0.91 V/Å, and the second is a result of (partial) energy relaxation. At 1.04 V/Å, the water molecules are being repelled off the surface. The charge-transfer involved with the repulsion is expressed by the charges provided in the table. The numbers at the right-hand side of each column correspond to the sum of the charges on the molecule.

water molecule to the reacting CO species. In this figure, the stable geometries arising from such coordination are shown as a function of the applied field. It is demonstrated that the water molecule below the 1.04 V/Å applied field remains lying above the layer in an unreactive position. Furthermore, at applied fields above this value, the water molecules are repelled off the surface toward the bulk of the solution.

In Table 1, we list the charges of the adsorbed atoms and the two Pt atoms used for the adsorption sites under the influence of the 1.04 V/Å applied potential. We also list (at the right side of each column) the total charge of the different CO and water molecules included in the model at two structures. The higher energy value is calculated using the optimized geometry at a smaller applied field (0.91 V/Å), whereas the second column corresponds to a geometry which was allowed to relax under the influence of the higher applied field of 1.04 V/Å. The application of the field does not seem to influence the charges of the CO species, which remain almost constant. Instead, it is shown that the water cluster is oxidized by transferring the negative charge to the surface atoms (not included in the table). The water cluster is driven off the surface by the applied gradient of the electric potential. Thus, at even much stronger fields, the water molecule is still not able to spontanously become reactive with the surface and the CO species remain unreacted.

Furthermore, we have attempted to identify a reactive PES which is physically reasonable at these conditions (full CO coverage). We have performed geometry optimization of perturbed structures at high potential bias. These perturbed structures are physically motivated guesses of the transition state leading to a reactive PES. The initial guess structure suggests proton transfer from the "attacking" water molecule to the hydrating molecules. In addition, the remaining OH is placed in close (and thus potentially reactive) proximity to the relaxed CO molecules. A scheme describing this structure is provided in Figure 2. The optimization has demonstrated that even at these conditions, which are highly favorable for oxidation to occur, the water molecule was reformed and has returned to the unreactive position as shown above in Figure 1. Thus, despite the limitations of the model, it is possible to provide prediction on the possibility of oxidation (not) to occur at full coverage conditions.

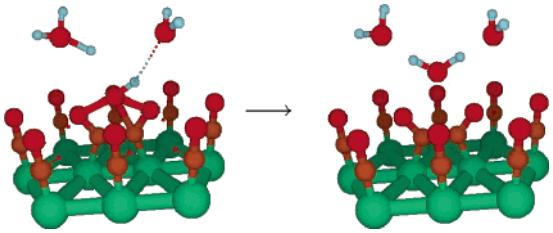

Figure 2. Reactive coordination of the water molecules above a full layer of CO is considered. The guess structure involves abstraction to the "bulk" of a hydrogen and a reactive placement of the remaining OH species adjacent to the CO layer. Even at these favorable conditions for the reaction to occur, upon geometry optimization under applied electric potential the unreactive water cluster is reformed.

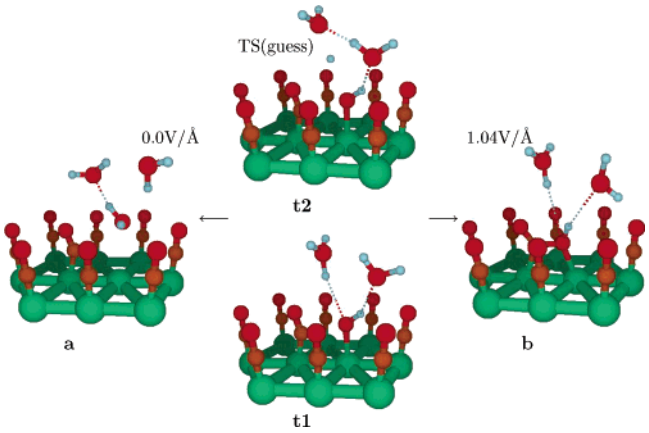

Figure 3. Extended models involving a vacancy. Two different types of optimized structures are obtained from a guess of a transition state (TS) conformation. The guessed TS (t2 or t1 in the figure) has water adsorbed as OH on the surface and a hydrogen being transferred toward the bulk. Upon optimization, at zero field, the water molecule is desorbed and reformed (a), whereas at strong field bias the formation of adsorbed COOH species is predicted (b).

We conclude, based on the models employed in this study, that the energy barrier for the reaction to occur at full coverage conditions cannot be small enough, even under the influence of strong applied electric potentials. Below, we will discuss other related surface scenarios, where the reaction can become more favorable above a certain applied electric potential.

Now, we will consider other possibilities apart from direct approach of the water molecule to the CO layer for the reaction to occur. Specifically, we allow a vacancy to occur next to an adsorbed CO on an atop site. We will discuss several variants of PESs which involve such vacancy. The first type is referred to as preoxidation PESs. In a preoxidation PES, the spatial geometries correspond to coordination of the reactive CO and water molecule before oxidation has taken place. The second type of PES is characterized as reactive. In a reactive PES, the reactive species involved in the reaction mechanism are already formed.

To highlight the geometrical features of both types of PESs, it is useful to consider Figure 3. The figure provides the result of geometry optimizations from a starting structure representing a guess for the transition state leading to the formation of the oxidized CO intermediate. In the guess structure, one water molecule reacts with the surface and loses a proton to the surrounding water molecules (denoted (t2) in the figure). Then, the optimization is performed at two extreme conditions. At one extreme, no potential bias is employed, and in the second case, a strong potential bias is incorporated. It is demonstrated that at zero electric potential bias upon optimization the water molecule is reformed and stays at an unreactive coordination

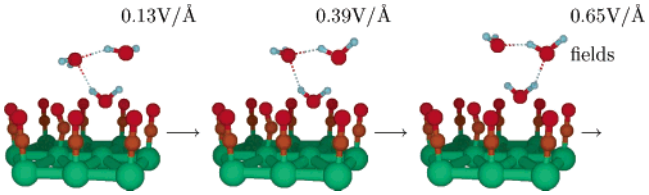

Figure 4. Extended models with one empty site. Geometries corresponding to a preoxidation PES are depicted. With the increase of the applied field, water approach the empty site as a preparation for the reaction. Water, at strong enough potential bias, will provide the required OH species for the reaction through dissociative adsorption to the empty site.

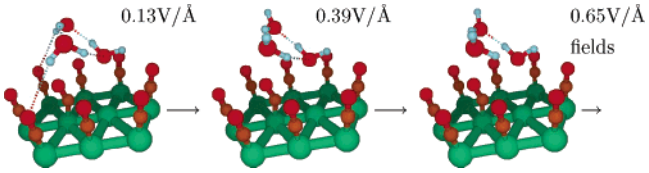

Figure 5. Extended models with one empty site. Geometries corresponding to an additional preoxidation PES are depicted. This PES differs from the previous preoxidation curve by the relative orientation of the water molecules. It involves orientation of one of the additional water molecules to point with its hydrogens toward the surface. This PES is less likely to promote CO oxidation than the previous PES.

above the surface (structure a). At the strong bias field, on the other hand, the COOH species, previously identified as an intermediate in the reaction,[10] is formed (structure b).

In addition, we have used other guess structures where the proton was further pushed to the more distanced water molecule. The result of using this guess (t1) as an initial guess at zero field also leads to the reformation and desorption of the water molecule. Thus, it is important to stress that, although we have employed only guesses of the transition states, the different optimized structures obtained at the extremes of the applied field properly demonstrate the effect of the bias field (within the cluster model approximation). Next we subject these two types of optimized geometries to the influence of varying potential bias to obtain the corresponding PESs and compare their energetics.

Figure 4 sketches the approach of water to the surface above the vacancy in preparation for the reaction to occur. This is the preoxidation PES. However, additional PESs not involving oxidation can be identified as well. Figure 5 provides sketches of such a PES. This PES differs in the relative orientation of the water molecules. In the previous PES, the oxygens of the two more distant water molecules are oriented to allow proton transfer from the reactive water molecule to the solution. This transfer is crucial for oxidation to occur. In the second PES, this is reversed and the proton transfer can occur to the CO species on the surface.

Figure 6 provides the energetical comparison of these PESs. It is demonstrated that at fields larger than 0.5 V/Å it becomes more stable to have all water molecules pointing down toward the surface with the oxygen. The comparison of these two PESs again suggests that the reactive coordination which leads to oxidation is related to a water molecule being first adsorbed on the surface and then undergoing dissociation. Similar conclusions have been drawn in the study of Narayanasamy and Andersson who employed more limited models and found that the direct attack of adsorbed CO by water molecules to be less favorable than the alternative route.[20]

Next, a reactive PES is included in the comparison as well. This PES becomes most stable at high enough applied potentials.

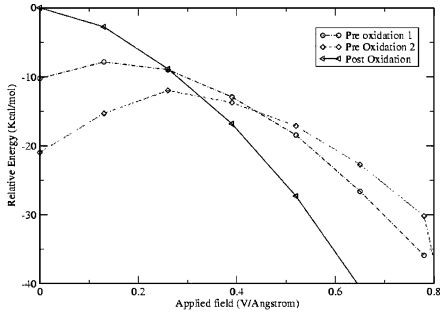

Figure 6. Relative stability of the different potential surfaces with a vacancy next to an adsorbed CO site. Two preoxidation PES are provided. The first (denoted as 1) involves favorable (for the reaction) orientation of the water molecule toward the vacancy. This PES becomes more stable than the second preoxidation PES at a certain potential bias. Note, the reactive PES becomes most stable above a similar applied bias field. Energies are provided in kcal/mol relative to the reactive PES at zero applied field.

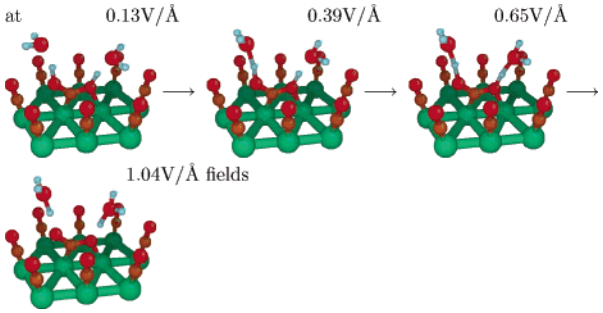

Figure 7. Extended models with one empty site. A post oxidation PES is depicted. A HO−C−OH species is shown to lose the hydrogens to produce CO_{2ads}. This reactive coordinate becomes more energetically stable than preoxidation coordinates at high enough applied fields.

Figure 7 sketches the geometries of a possible PES where oxidation of CO has already occurred. The reactive PES has been modified from the one discussed above to describe a possibly more stable configuration especially at low potentials. Accordingly, H_2O is still dissociatively adsorbed in the form of OH on the surface and hydrogen atom transfer. However, the proton is transferred to the neighbor adsorbed CO molecule. This introduces a variant of the previously oxidized CO intermediate species, a di-hydrogenated species (HO−C−OH). In the figure (Figure 7), it is demonstrated that HO−C−OH under the influence of electric potential bias will lead to the final product of CO oxidation, a CO_2 molecule. In this PES, the two protons are released to the solution through the two additional water molecules included in the model.

Table 2 provides insight into the occurrence of the reaction. The table lists the charges of the adsorbed species HO−C−OH (and the hydrogens and the CO_2 molecule separately) as a function of the applied potential. $(HO-C-OH)_{ads}$ becomes more positively charged as the applied field is increased. In addition, the charges on the hydrogens suggest that the overall reaction is a composite of dehydrogenation and deprotonation processes.

Figure 6 provides the energetical comparison of the PESs. The relative stability of the PESs depends on the applied external field. As discussed above, at low potential bias the reacted conformation lies higher in energy than the preoxidation curves. However, the same PES becomes more stable at above a certain applied potential bias. Thus, the occurrence of the oxidation process becomes more favorable. The entropic contributions of the different related adsorbates are not expected to depend strongly on the applied electric potential. We have performed model calculations of adsorbed CO, CO_2, and positively charged

TABLE 2: Charges of the HO−C−OH Species Formed on the Surface with Respect to the Change in the Applied Field in the Reactive PES Involving a Vacancy[a]

	partial charges (a.u.)		
field (V/Å)	COHOH	H H	COO
0.0	0.2906	1.0194	−0.7288
0.13	0.3148	1.0379	−0.7231
0.26	0.3380	1.0559	−0.7179
0.39	0.3540	1.0698	−0.7158
0.52	0.3756	1.0826	−0.7071
0.65	0.3923	1.0831	−0.6909
0.78	0.4112	1.0898	−0.6786
0.91	0.4254	1.0895	−0.6641
1.04	0.4729	1.0865	−0.6135
1.17	0.4978	1.0865	−0.5888

[a] The species is charged more positively as the strength of the applied field increases. The charges of the hydrogen atoms are slightly above 0.5 a.u., which indicates the process being a hybrid of deprotonation and hydrogenation.

diprotonated CO_2 intermediates bonded to a single Pt atom for the entropy within the harmonic oscillator approximation. We found the different adsorbate entropy dependence on the electric field to be vanishing. Thus, we do not expect the picture provided by the PESs as described above to change by entropy considerations.

Full mapping of these PESs including the calculation of energetical barrier and transition geometries separating the different surfaces is a desired refinement which will lead to further understanding of the system. Thus, it is important to note a limitation of the models used in this work as observed in the results. The preoxidation conformations at 0.91 V/Å exhibit an aligned conformation of the three water molecules. The water molecules at this bias create a positively charged cluster which is being infinitely drawn to the solution "bulk" away from the surface. The aligned water cluster conformation, however, is clearly not what we intended to simulate in the calculation. This is a manifestation of the limitations imposed by the approximations introduced in the model. Addressing these problems will be crucial when full mapping of the PESs is desired.

Conclusions

Cluster models of Pt(111) surface electrodes are used to gain insight on the CO electrooxidation process. Applied electric potentials are simulated by local fields. These simple models are able to describe CO electrooxidation trigerred by potential bias via the formation of hydrogenated CO_{2ads} as the reaction intermediate species. These species lose their hydrogens under the influence of an applied field.

In this study, we have concentrated on the question of how such a reaction can start when full coverage of the surface is considered. We have extended the basic cluster model to qualitatively represent a surface with a full cover of adsorbed CO. Thus, the starting point of the extended model involves only CO molecules as adsorbates, whereas the oxygen containing species has to be formed under the influence of the potential bias from the surrounding water molecules. It is suggested that a vacancy (or a surface defect) adjacent to the reacting adsorbed CO is needed to facilitate the reaction at moderate applied electric potentials. According to our calculations, a full layer of CO inhibits the possibility of a reaction with water molecules even at strong applied potential. This is in agreement with the experimental study of Lebedeva et al. on the influence of defects on the kinetics of CO electrooxidation.[22] It was demonstrated that the experimental rate constant for the reaction should be zero if an "ideal" Pt(111) electrode could be used.

Furthermore, it is suggested that the reaction can be initiated by a dissociative adsorption of water at an adjacent site to one with adsorbed CO. This results in the formation of a hydrogenated CO oxidation intermediate. The current study introduces a di-hydrogenated variant of the previously suggested intermediate as another possible route for the reaction to follow. These two variants differ by the result of the proton-transfer originating from the dissociative adsorption of water. The hydrogen can either transfer to the "bulk" solution to leave a COOH adsorbate or migrate on the surface to yield a di-hydrogenated adsorbed species, HO−C−OH. It is a desired future refinement to establish which species or route is more favorable. However, such refinement will not modify our current conclusion that in order for the reaction to occur a vacancy next to adsorbed CO must become available to allow the reaction to proceed. The formation of CO_2 is readily obtained via proton transfer(s) under the influence of the potential bias.

Acknowledgment. This work was partially supported by a grant from the National Science Foundation (CHE-9981977), with additional partial support from the Director, Office of Energy Research, Office of Basic Energy Sciences, Chemical Sciences Division, of the U.S. Department of Energy, under Contract DE-AC03-76SF00098. A grant of supercomputer time at NERSC was used to perform the computations reported here.

References and Notes

(1) Gilman, P. *J. Phys. Chem.* **1964**, *68*, 70.
(2) Gasteiger, H. A.; Markovic, N. M.; Ross, P. N.; Cairns, E. J. *J. Phys. Chem.* **1994**, *98*, 617.
(3) Anderson, A. B.; Grantscharova, E. *J. Phys. Chem.* **1995**, *99*, 9149.
(4) Koper, M. T. M.; Jansen, A. P. J.; van Santen, R. A.; Lukkien, J. J.; Hilbers, P. A. J. *J. Chem. Phys.* **1998**, *109*, 6051.
(5) Saravanan, C.; Koper, M. T. M.; Markovic, N. M.; Head-Gordon, M.; Ross, P. *Phys. Chem. Chem. Phys.* **2002**, *4*, 2660.
(6) Feibelman, P. J.; Hammer, B.; Norskov, J. K.; Wagner, F.; Scheffler, M.; Stumpf, R.; Watwe, R.; Dumesic, J. *J. Phys. Chem. B* **2001**, *105*, 4018.
(7) Christofferson, E.; Liu, P.; Ruben, A.; Skriver, H. L.; Norskov, J. K. *J. Catal.* **2001**, *199*, 123.
(8) Koper, M. T. M.; Shubina, T. E.; van Santen, R. A. *J. Phys. Chem. B* **2002**, *106*, 686.
(9) Anderson, A. B.; Neshev, N. M. *J. Electrochem. Soc.* **2002**, *149*, E383.
(10) Saravanan, C.; Dunietz, B.; Markovic, N.; Somorjai, G.; Ross, M. P. N. M. Head-Gordon. *J. Electroanal. Chem.* **2003**, *554−555*, 459.
(11) Becke, A. *J. Chem. Phys.* **1993**, *98*, 1372.
(12) Becke, A. *J. Chem. Phys.* **1993**, *98*, 5648.
(13) Wadt, W. R.; Hay, J. P. *J. Chem. Phys.* **1985**, *82*, 299.
(14) Kong, J.; White, C. A.; Krylov, A. I.; Sherrill, C. D.; Adamson, R. D.; Furlani, T. R.; Lee, M. S.; Lee, A. M.; Gwaltney, S. R.; Adams, T. R.; Ochsenfeld, C.; Gilbert, A. T. B.; Kedziora, G. S.; Rassolov, V. A.; Maurice, D. R.; Nair, N.; Shao, Y.; Besley, N. A.; Maslen, P. E.; Dombroski, J. P.; Dachsel, H.; Zhang, W. M.; Korambath, P. P.; Baker, J.; Byrd, E. F. C.; Voorhis, T. V.; Oumi, M.; Hirata, S.; Hsu, C. P.; Ishikawa, N.; Florian, J.; Warshel, A.; Johnson, B. G.; Gill, P. M. W.; Head-Gordon, M.; Pople, J. A. *J. Comput. Chem.* **2000**, *21*, 1532.
(15) Bagus, P. S.; Nelin, C. J.; Muller, W.; Philpott, M. R.; Seki, H. *Phys. Rev. Lett.* **1987**, *58*, 559.
(16) Head-Gordon, M.; Tully, J. C. *Chem. Phys.* **1993**, *175*, 37.
(17) Koper, M. T. M.; van Santen, R. A.; Wasileski, S. A.; Weaver, M. J. *J. Chem. Phys.* **2000**, *113*, 4392.
(18) Chou, K. C.; Markovic, N. M.; Kim, J.; Ross, P.; Somorjai, G. A. *J. Phys. Chem. B.* **2003**, *107*, 1840.
(19) Chou, K. C.; Kim, J.; Baldelli, S.; Somorjai, G. A. *J. Electroanal. Chem.* **2003**, *554−555*, 253.
(20) Lebedeva, N. P.; Koper, M. T. M.; Feliu, J. M.; van Santen, R. A. *J. Electroanal. Chem.* **2002**, *524−525*, 242.
(21) Narayanasamy, J.; Anderson, A. *J. Electroanal. Chem.* **2003**, *554−555*, 35.
(22) Lebedeva, N. P.; Koper, M. T. M.; Feliu, J. M.; van Santen, R. A. *J. Phys. Chem. B.* **2002**, *106*, 12938.